Supplemental information

Supplementary Figure Legends

Supplementary Table 1. Genotypes of Yeast Strains Used in This Study

All strains are MAT**a** *ura3-1, his3-11,15, leu2-3,112, trp1-1, RAD5*. * CEB1 placed in orientation I. ** CEB1 placed in orientation II (illustrated in Figure 1C).

Supplementary Table 2. Rearrangement Frequencies of CEB1 Alleles of Various Sizes in Orientation I in *pif1Δ* Cells

Supplementary Table 3. Localization of G-Quadruplex-Forming Sequences Relatively to Surrounding Early-Firing Replication Origins.

G-quadruplex-forming (G4F) sequences ($G_3N_{1-9}G_3N_{1-9}G_3N_{1-9}G_3$) list have been determined using Quadparser (Huppert and Balasubramanian, 2005) and manually curated to eliminate telomeric G-quadruplex-forming sequences. Strand of the G-quadruplex-forming sequence is indicated (+ is Watson and – is Crick strand). Coordinates of the closest early-firing origins (Fachinetti et al., 2010) in 5' and in 3', as well as the distance to each G4F sequence, are indicated.

Supplementary Figure 1. ARS Location and Replication Dynamics in the 120 kb Region Surrounding the *ARS305* Region of Chromosome III

The CEB1 insertion site, near *ARS305* is shown. Replication profiles were obtained from the DNA Replication Origin Database website (http://www.oridb.org) (Nieduszynski et al., 2007). Black arrows indicate active origins. Grey arrows indicate inactive or poorly active ARS.

Supplementary Figure 2. Viability of WT, *pif1Δ*, *rad51Δ* and *pif1Δ rad51Δ* Cells with CEB1-1.8 in the Orientation I and II

(**A**) At t=0, budded cells from an exponentially growing culture are put on a grid by micromanipulation on a YPD plate. After 1-3h, mother and daughter cells are separated and put in the adjacent coordinate on the grid (for more details, see Supplementary Methods). Cells that failed to separate after 3 hours on plate were removed of the analysis. The number of colonies formed by each pairs of cells (0, 1, or 2 colonies) is counted after 3 days of growth at 30°C, and the results are reported in (**B**). (**B**) Percentage of separated pairs of cells that gave rise to 0, 1, or 2 colonies. The strains are the same as in Table 1. The control *pif1Δ* strain without CEB1 insert is ORT6133-2 (see Supplementary Table 1). Number of pairs analyzed, as well as the percentage of viable cells, are indicated. Statistical significance was calculated by comparing the distributions of pairs in the 0, 1, and 2 colonies categories with the Fischer exact test (α cutoff of 0.05).

Supplementary Figure 3. Cell Cycle Progression Analysis by FACS After α-Factor Synchronisation

(**A**) The WT ORT6119-4 (orientation I), ORT6135-36 (orientation II) cells and the *pif1Δ* ORT6123-1-5 (orientation I), ORT6136-8 (orientation II) cells were arrested in G1 by α-factor treatment and release into fresh medium. Samples were collected at the indicated time points (minutes) for FACS analysis and 2G-gels electrophoresis (Figure 4A).

(**B**) Cell cycle progression of the synchronized *pif1Δ* strain (ORT6157-1) with the CEB1-Gmut-1.7 in orientation I. Other legends as in (A). The 2D-gel electrophoresis is presented in Figure 4B.

(**C**) Cell cycle progression of the synchronized WT ORT6119-4 (orientation I) and ORT6135-36 (orientation II) cells treated or not with 10 μM Phen-DC_3. In the Phen-DC_3-treated samples, the shift from the 1C to 2C peak is slightly delayed compared to the control sample. Other legends as in (**A**). The 2D-gel electrophoresis is presented in Figure 4D.

(**D**) Cell cycle progression of the synchronized *pif1Δ* (ORT6123-1-5) and *pif1Δ rad51Δ* (ORT6139-5) and *pif1Δ rad52Δ* (ORT6153-2) cells carrying CEB1 in the orientation I. Other legends as in (**A**). The 2D-gel electrophoresis is presented in Figure 4F.

Supplementary Figure 4. Recombination-intermediates Formation during S-phase Seems Associated With Fork Pausing

(**A**) Time course analysis by 2D-gel electrophoresis of DNA intermediates formed in CEB1 arrays in orientation I during S-phase in synchronized WT (ORT6119-4) and *pif1Δ* (ORT6123-1-5) cells. Restriction digests and expected DNA fragment sizes for CEB1 in the orientation I (HaeII/SacII and ApaI/SpeI) are shown in the top panel. Progressive doubling of the signal intensity is expected to occur in the descending part of the Y arc (large Y) with the HaeII/SacII digest in WT and *pif1Δ* cells (see also Figure 4A). With the ApaI/SpeI digest in *pif1Δ* cells, the accumulation of signal in the ascending part of the Y arc (small Y), associated with the decrease of the large Y arc signal, suggests fork pausing inside the CEB1-G-quadruplex repeats. Blue lines outline CEB1 position in the Y arc. Other legends as in Figure 4A.

(**B**) Time course analysis by 2D-gel electrophoresis of DNA intermediates formed in CEB1-Gmut-1.7 in orientation I during S-phase in a *pif1Δ* strain (ORT6157-1). Genomic DNA were digested with HaeII/ApaI or SpeI. Contrary to the *pif1Δ* cells with CEB1 G-quadruplex-prone sequence, the signal of replication intermediates remains in the decending part of the Y arc even with the SpeI digest, suggesting that the absence of G-quadruplex-forming sequence abolishes the replication fork pausing. Other legends as in Figure 4B.

(**C**) Relative time course quantification of the large and small Y arc signals observed in experiments A and B. Left panel: Ratio of large Y / small Y with CEB1 located in the descending part of the Y arc (HaeII/SacII and HaeII/ApaI digests). Right panel: Ratio of large Y / small Y with CEB1 located in the ascending part of the Y arc (ApaI/SpeI and SpeI digests).

Supplementary Figure 5. Sequence Analysis of the CEB1 Rearrangements Induced by Phen-DC_3 in WT cells

Schematic representation of the polymorphic motif structure of the parental CEB1-1.8 allele and of 24 contractions obtained in WT strains carrying CEB1-1.8 array in the orientation I and II (strains ORT6119-4 and ORT6135-36, respectively) treated with 10 μM of Phen-DC_3. Among the 43 motifs in the natural CEB1-1.8 allele, 25 can be distinguished by one or several polymorphisms (Lopes et al., 2006) that have been used to determine the more likely structure of the rearrangements. The rearrangements felt into 3 categories: simple-deletion, double-deletion, and complex reshuffling of the parental sequence. The three classes of rearrangements are generated independently of CEB1 orientation. White motif in II-C1 contains polymorphisms of at more than 2 parental motifs.

Supplementary methods

Yeast strain construction

All yeast strains used in this study were built by transformation of the parental SY2209 *Saccharomyces cerevisiae* strain of the W303 background (Fachinetti et al., 2010). Their genotypes are reported in Supplementary Table 1. The introduction of the CEB1 arrays near the *ARS305* locus was performed in several steps. First, the *URA3* marker was inserted on Chr. III in the intergenic region between the divergent *YCL048w*-*YCL049c* genes, between positions 41801-41840 (Cherry et al., 1997). This insertion was obtained by lithium-acetate transformation of the SY2209 strain with a PCR product constructed to provide sufficient flanking homology: i.e. containing an upstream fragment of 385 bp (from 41416 to 41801 on Chr. III), the *URA3* gene amplified from pRS416 and a downstream fragment of 412 bp (from 41840 to 42252 on Chr. III). It generated strain ORT5094-1. Then, the Hygromycin resistant marker (*HphMX4*) (Goldstein and McCusker, 1999) from pMJ696 was inserted in ORT5094-1 between positions 41841 and 41900 on Chr. III by long flanking homology transformation to yield ORT6143-13. Then, this strain carrying the *URA3* and *HphMX4* genes in close proximity was used to introduce the CEB1 minisatellite arrays (CEB1-1.8 orientation I, CEB1-1.8 orientation II or CEB1-Gmut-1.7) using PCR products containing the desired CEB1 allele and appropriate Chr. III flanking regions to substitute the markers and introduce CEB1. Sequentially, the transformants of strain ORT6143-13 were selected on 5FOA media (selecting *ura*- strains) and then screened for Hygromycin sensitivity. The CEB1-containing PCR products were constructed as follows. The flanking upstream fragment of 385 bp (from 41416 to 41801 on Chr. III) was amplified from yeast genomic DNA with a couple of primers, each containing a terminal ApaI restriction site. The PCR product digested by ApaI was inserted into pJL80 (pUC19 derivated plasmid containing the CEB1-1.8 orientation I) to create plasmid pJL115. Then, the downstream fragment of 412 bp (from 41840 to

42252 on Chr. III) was amplified with two primers to add terminal XhoI and AflII sites, and inserted into pJL115 to create pJL116. The Bsu36I/AflII fragment from pJL116 carrying the CEB1-1.8 minisatellite (orientation I) flanked by the Chr. III regions was used for transformation of the ORT6143-13 strain to produce ORT6119-4 in which the CEB1 allele is cleanly inserted, without additional marker that may generate transcriptional interference with replication. Homologous integration was verified by Southern blot analysis of the transformants. Similarly, an upstream 385 bp XhoI/SacII and downstream 412 bp ApaI/AflII chr. III fragments were successively integrated into pJL85 (pUC19 derivated plasmid with CEB1-1.8 orientation II) to create plasmid pJL122. The XhoI/AflII fragment from pJL122, was used to transform ORT6143-13 resulting in ORT6135-36. To insert the CEB1-Gmut-1.7 array near *ARS305*, it was amplified from plasmid pPA58-4 (pGEM®-T Easy vector (Promega) containing CEB1-Gmut-1.7 minisatellite) with primers adding terminal SacII and ApaI restriction sites and cloned in pJL122 to replace the CEB1-1.8 minisatellite by the CEB1-Gmut-1.7. The resulting plasmid, pJL125, was digested by XhoI/AflII and used to transform ORT6143-13 resulting in ORT6582-4. All transformants were verified by Southern blot analysis of genomic DNA allowing for the confirmation of the markers loss and their replacement by the expected CEB1 array. Inactivation of the *PIF1*, *RAD54*, *REV1*, *RRM3*, and *SGS1* genes with the selectable *KanMX4* marker (G418 resistance) were obtained by transformation of the ORT6119-4 and ORT6135-36 strains with PCR products amplified from the corresponding strains of the EUROSCARF deletants collection (Winzeler et al., 1999). Similarly, the *pif1::HIS3, rad27::HIS3, rad51::LEU2* and *rad52::LEU2* disruptions were obtained by transformation with PCR products from strains ORD9922-4B, ORD6713-8D, ORD7574-9B and ORD7565-2C, respectively (Ribeyre et al., 2009). Double mutant strains were similarly constructed by transformation of single mutant strains. ORT6146-1 and ORT6136-8 were both transformed by the PCR products *rad51::LEU2* and *rad52::LEU2*. The *pif1-K264A* point mutation was introduced at the *PIF1* locus by pop-in and pop-out transformation (Scherer and Davis, 1979) of ORT6119-4 and ORT6135-36, as previously described (Ribeyre et al., 2009). To build the deletion of *ARS305*, plasmid pMJ593 (Dershowitz et al., 2007) containing the *ARS305* deletion (1100 bp deletion of BamHI-ClaI fragment, from 38606 to 39706 on Chr. III) plus the flanking regions (3' end of *YCL51W* and the 5' end of YCL48W), was linearized by HpaI and integrated by pop-in pop-out transformation of ORT6119-4 and ORT6135-36. For all transformants, integration at the homologous locus was verified by Southern blot analyses of genomic DNA using appropriate restriction digest and probes flanking the targeted locus.

Supplementary references

Cherry, J.M., Ball, C., Weng, S., Juvik, G., Schmidt, R., Adler, C., Dunn, B., Dwight, S., Riles, L., Mortimer, R.K. and Botstein, D. (1997) Genetic and physical maps of Saccharomyces cerevisiae. *Nature*, 387, 67-73.

Dershowitz, A., Snyder, M., Sbia, M., Skurnick, J.H., Ong, L.Y. and Newlon, C.S. (2007) Linear derivatives of Saccharomyces cerevisiae chromosome III can be maintained in the absence of autonomously replicating sequence elements. *Mol Cell Biol*, 27, 4652-4663.

Goldstein, A.L. and McCusker, J.H. (1999) Three new dominant drug resistance cassettes for gene disruption in Saccharomyces cerevisiae. *Yeast*, 15, 1541-1553.

Nieduszynski, C.A., Hiraga, S., Ak, P., Benham, C.J. and Donaldson, A.D. (2007) OriDB: a DNA replication origin database. *Nucl. Acids Res.*, 35, D40-46.

Scherer, S. and Davis, R.W. (1979) Replacement of chromosome segments with altered DNA sequences constructed in vitro. *Proc Natl Acad Sci U S A*, 76, 4951-4955.

Winzeler, E.A., Shoemaker, D.D., Astromoff, A., Liang, H., Anderson, K., Andre, B., Bangham, R., Benito, R., Boeke, J.D., Bussey, H., Chu, A.M., Connelly, C., Davis, K., Dietrich, F., Dow, S.W., El Bakkoury, M., Foury, F., Friend, S.H., Gentalen, E., Giaever, G., Hegemann, J.H., Jones, T., Laub, M., Liao, H., Liebundguth, N., Lockhart, D.J., Lucau-Danila, A., Lussier, M., M'Rabet, N., Menard, P., Mittmann, M., Pai, C., Rebischung, C., Revuelta, J.L., Riles, L., Roberts, C.J., Ross-MacDonald, P., Scherens, B., Snyder, M., Sookhai-Mahadeo, S., Storms, R.K., Veronneau, S., Voet, M., Volckaert, G., Ward, T.R., Wysocki, R., Yen, G.S., Yu, K., Zimmermann, K., Philippsen, P., Johnston, M. and Davis, R.W. (1999) Functional characterization of the S. cerevisiae genome by gene deletion and parallel analysis. *Science*, 285, 901-906.

Supplementary Figure 1

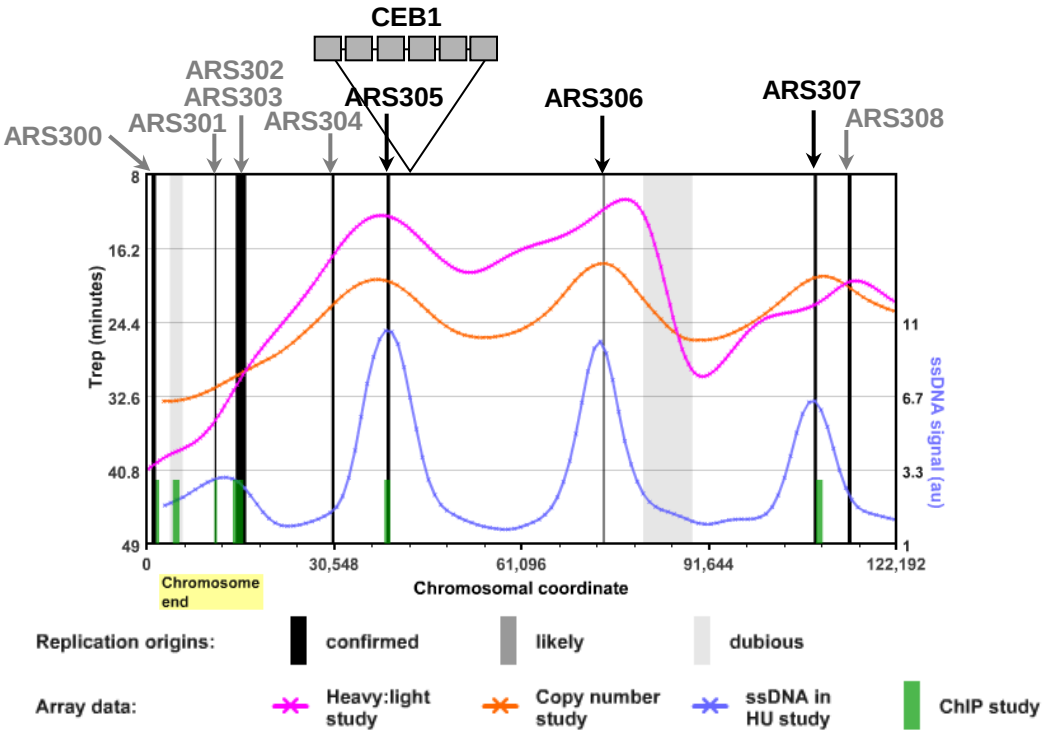

Supplementary Figure 2

A

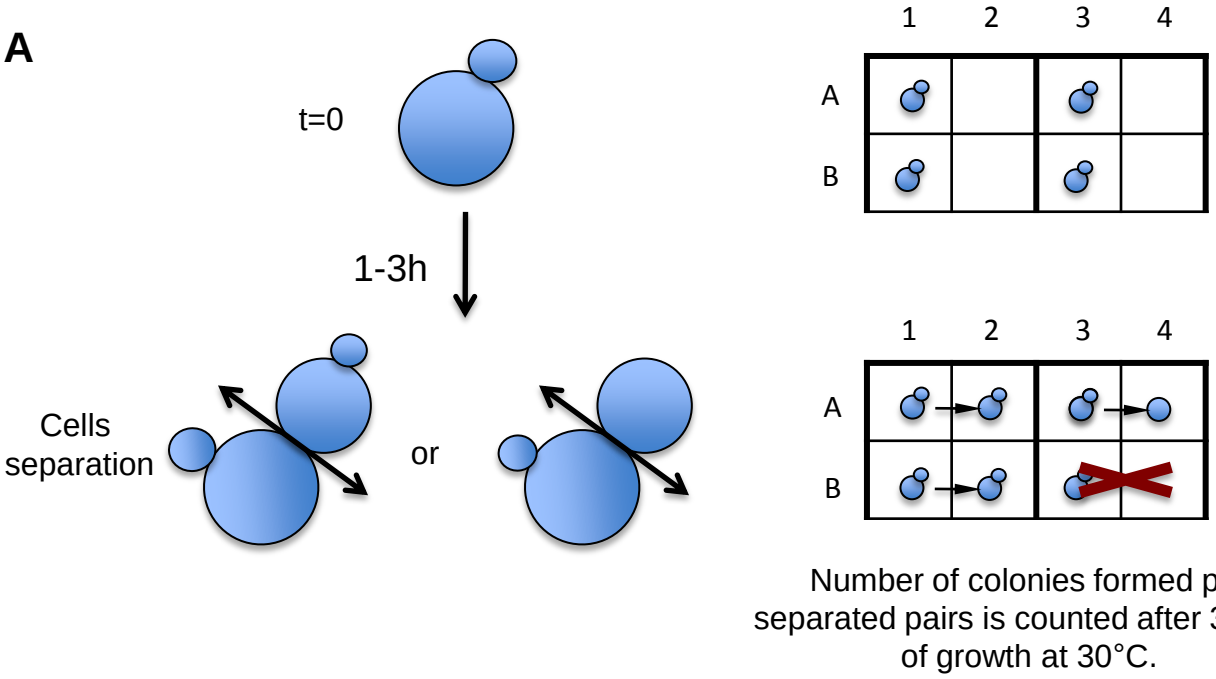

Number of colonies formed per separated pairs is counted after 3 days of growth at 30°C.

B

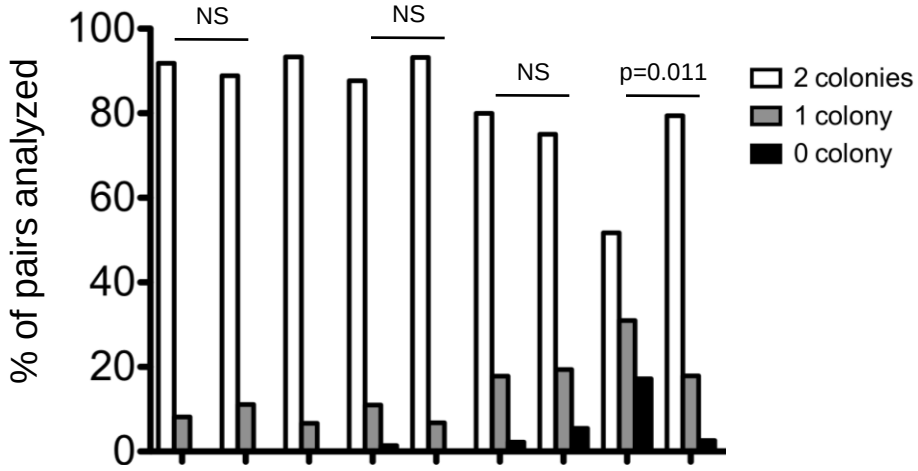

Pairs analyzed:	49	27	30	73	44	45	36	58	39
Viable cells (%):	96	94	97	93	97	89	85	67	88
CEB1 orientation:	I	II	-	I	II	I	II	I	II
Genotype:	WT		*pif1Δ*			*rad51Δ*		*pif1Δ rad51Δ*	

p-values (Fischer exact test)	**Orientation I**	**Orientation II**
rad51Δ vs. *pif1Δrad51Δ*	$5.9e^{-3}$	0.82
pif1Δ vs. *pif1Δrad51Δ*	$7.5e^{-6}$	0.13

Fig. S3

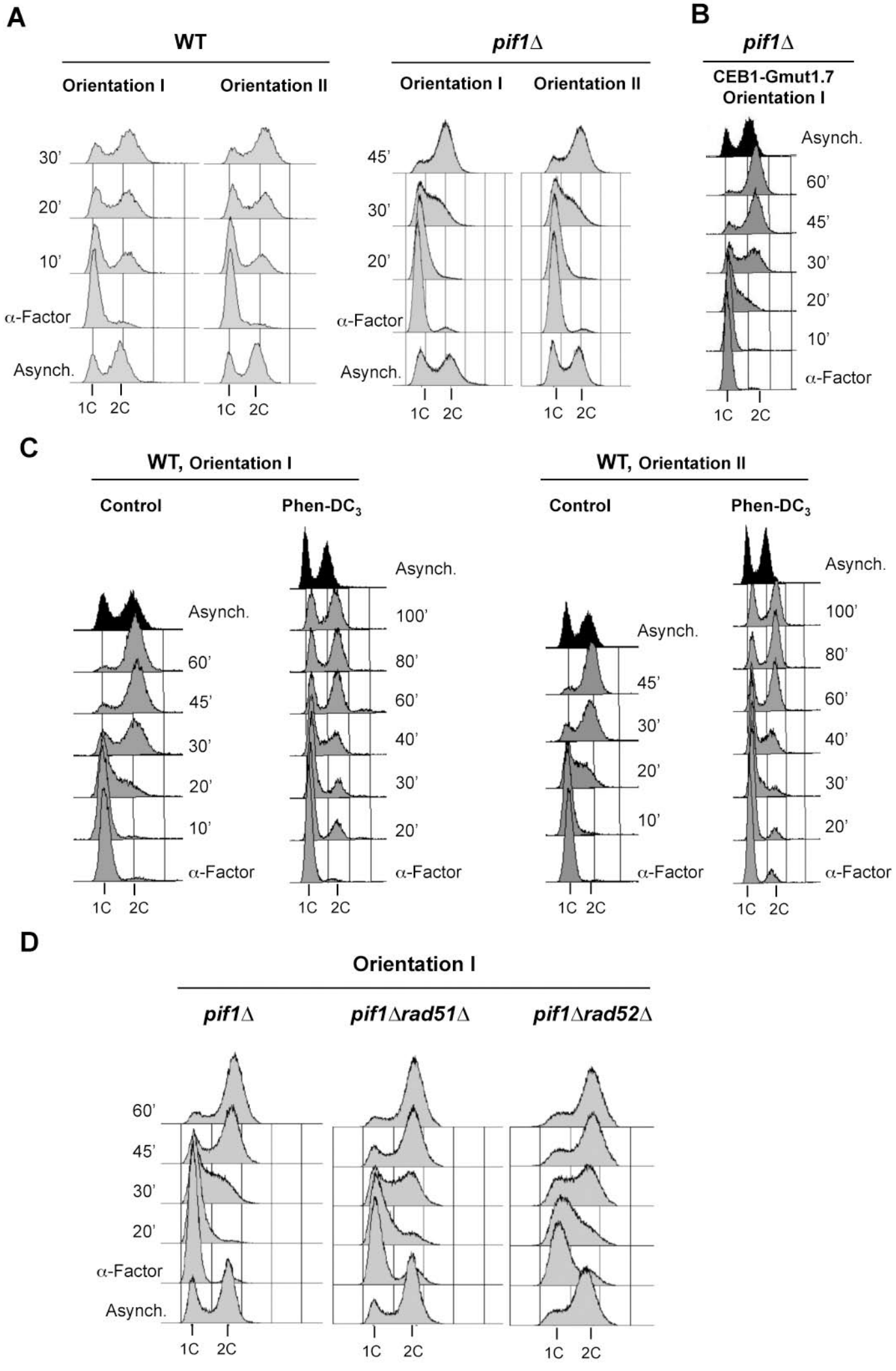
A
WT
Orientation I
Orientation II
30'
20'
10'
α-Factor
Asynch.
1C 2C
pif1Δ
Orientation I
Orientation II
45'
30'
20'
α-Factor
Asynch.
1C 2C
B
pif1Δ
CEB1-Gmut1.7
Orientation I
Asynch.
60'
45'
30'
20'
10'
α-Factor
1C 2C
C
WT, Orientation I
Control
Phen-DC3
Asynch.
60'
45'
30'
20'
10'
α-Factor
100'
80'
60'
40'
30'
20'
1C 2C
WT, Orientation II
Control
Phen-DC3
Asynch.
45'
30'
20'
10'
α-Factor
100'
80'
60'
40'
30'
20'
1C 2C
D
Orientation I
pif1Δ
pif1Δrad51Δ
pif1Δrad52Δ
60'
45'
30'
20'
α-Factor
Asynch.
1C 2C

Fig. S4

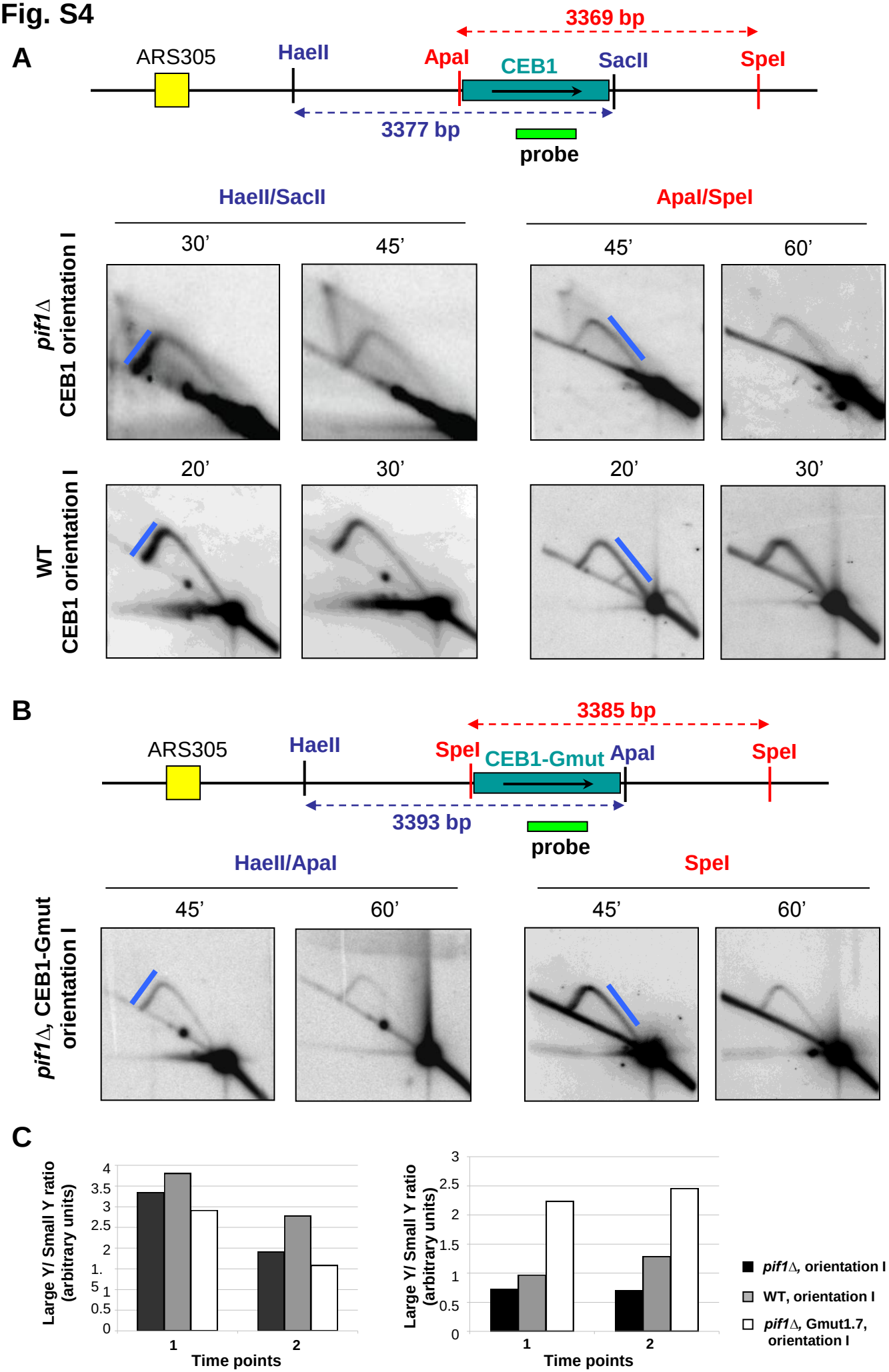
A
ARS305
HaeII
ApaI
CEB1
SacII
SpeI
3369 bp
3377 bp
probe
HaeII/SacII
ApaI/SpeI
pif1Δ CEB1 orientation I
30'
45'
45'
60'
WT CEB1 orientation I
20'
30'
20'
30'
B
ARS305
HaeII
SpeI
CEB1-Gmut
ApaI
SpeI
3385 bp
3393 bp
probe
HaeII/ApaI
SpeI
pif1Δ, CEB1-Gmut orientation I
45'
60'
45'
60'
C
Large Y/ Small Y ratio (arbitrary units)
Time points
pif1Δ, orientation I
WT, orientation I
pif1Δ, Gmut1.7, orientation I

Supplementary Figure 5

Parental CEB1-1.8

Orientation I

Deletions (n=6/12)

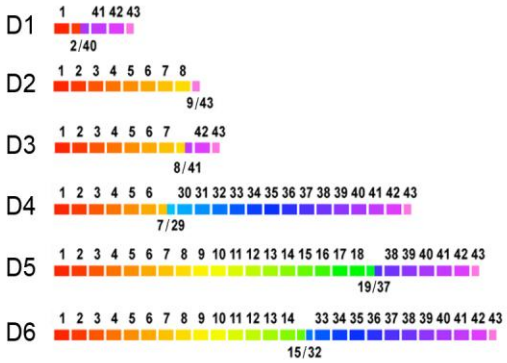

Double-deletions (n=3/12)

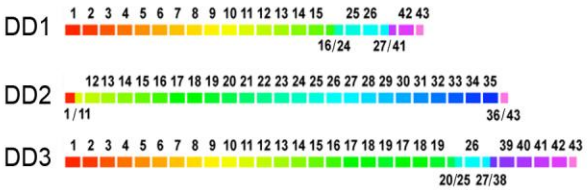

Complex (n=3/12)

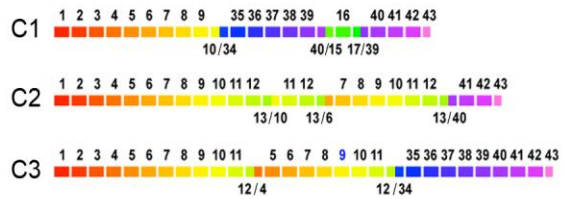

Orientation II

Deletions (n=8/12)

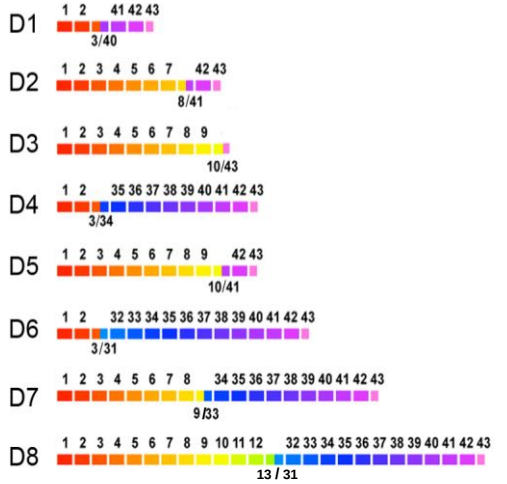

Double-deletions (n=1/12)

Complex (n=3/12)